Hindawi Publishing Corporation
Journal of Spectroscopy
Volume 2015, Article ID 714396, 8 pages
http://dx.doi.org/10.1155/2015/714396

Research Article

Spectroscopic Analysis of Heterogeneous Biocatalysts for Biodiesel Production from Expired Sunflower Cooking Oil

Enoch Wembabazi,[1] Patrick Joram Mugisha,[2] Asumani Ratibu,[2] Deborah Wendiro,[2] Joseph Kyambadde,[1] and Peter California Vuzi[1]

[1]*Department of Biochemistry and Sports Science, Makerere University, P.O. Box 7062, Kampala, Uganda*
[2]*Department of Product Development, Uganda Industrial Research Institute, P.O. Box 7086, Kampala, Uganda*

Correspondence should be addressed to Peter California Vuzi; pvuzi@cns.mak.ac.ug

Received 29 July 2015; Revised 20 November 2015; Accepted 22 November 2015

Academic Editor: Feride Severcan

The study characterized heterogeneous biocatalyst synthesized from sucrose, saw dust, and chicken egg shells using Fourier Transform Infrared (FTIR) spectroscopy coupled with Attenuated Total Reflectance (ATR) technique. Acidic sulphonate ($-SO_3H$) groups were more visible in the spectrum generated for carbonized and sulphonated sucrose than in carbonized and sulphonated saw dust. This was highlighted further by the significantly higher conversion percentage achieved for sulphonated sucrose (62.5%) than sulphonated saw dust (46.6%) during esterification of expired sunflower oil ($p = 0.05$). The spectra for calcinated egg shells also showed that the most active form of calcium oxide was produced at calcination temperature of 1000°C. This was confirmed in the single-step transesterification reaction in which calcium oxide generated at 1000°C yielded the highest biodiesel (87.8%) from expired sunflower oil. The study further demonstrated the versatility of the FTIR technique in qualitative analysis of biodiesel and regular diesel by confirming the presence of specific characteristic peaks of diagnostic importance. These findings therefore highlight the potential of FTIR-ATR as an inexpensive, fast, and accurate diagnostic means for easy identification and characterization of different materials and products.

1. Introduction

Several methods are currently employed in the study of materials, including X-ray fluorescence (XRF), X-ray diffraction (XRD), and scanning electron microscopy (SEM). However, these methods have several disadvantages including high cost of analysis per sample, relatively large sample requirement, low reproducibility, and safety concerns with use of X-ray equipment [1, 2]. Further, sample analysis using these techniques is tedious with lengthy sample preparatory steps, which makes working on large samples laborious [2].

These problems could be significantly reduced by using Fourier transform infrared spectroscopy (FTIR), a rapid, simple, and economic tool for studying materials, catalytic activity, and products from chemical reactions [3]. Besides, this technique is precise and nondestructive, requires small samples, is easily reproducible, has less need for messy chemicals, and permits the qualitative and quantitative identification of components in solids and liquids [4, 5].

Infrared spectroscopy may be defined as the triggering of vibrations in molecules of a sample through irradiation with infrared light, with the aim of producing a finger print of the sample with absorption peaks which correspond to bonds between the atoms that make up the molecule [6]. The intensity and wavelength of radiation absorbed or transmitted can be measured, thus providing a basis for detection and quantification of functional groups and molecules [7].

The use of FTIR spectroscopy for analyzing catalytic activity is increasingly becoming popular since it can identify chemical bonds in molecules by producing their infrared spectra [8], thus being deemed suitable for verifying presence of desired functional groups in catalysts or for structure elucidation [3]. Coupled with an attenuated total reflectance (ATR) accessory, the technique shortens the time of sample

preparation and eases spectral reproducibility, thus making sample analysis faster.

Previous investigators have successively used FTIR spectroscopy to characterize both homogeneous and heterogeneous catalysts [9, 10]. For instance, Engin et al. [11] first demonstrated the effect of different calcination temperatures on heterogeneous biocatalysts from egg shells using FTIR spectroscopy and were able to identify the key functional groups involved. Another study indicated the use of FTIR-ATR spectroscopy to identify acidic catalytic $-SO_3H$ groups on sulfonated biochar catalyst, with great ease [12], thus illustrating the wide applicability of this method in studying catalyst activity [9].

However, few studies have demonstrated FTIR-ATR spectroscopy as a stand-alone analytical tool for characterization and selection of catalysts and characterization of reactants and products of transesterification. Moreover, there is a growing need for rapid and simple tools for analysis of fatty acid methyl esters in the production chain of biodiesel industries [5]. The objective of this study was to show the ability of FTIR-ATR spectroscopy as a rapid and reproducible qualitative analytical tool of liquids and solids that could replace the more laborious official methods such as gas chromatography, X-ray fluorescence, and X-ray diffraction spectroscopy in qualitative analysis.

In this study, three heterogeneous biocatalysts synthesized from locally available materials, namely, chicken eggshells, sucrose, and saw dust, were characterized using FTIR-ATR spectroscopy in the midinfrared region to investigate their catalytic potential. Subsequently, the catalysts were employed in single-step transesterification and esterification reactions using expired sunflower oil. The biodiesel produced from the single-step transesterification and regular diesel from a local filling station were similarly analyzed using FTIR-ATR spectroscopy for diagnostic purposes as well as identification of differences between the two products.

2. Materials and Methods

2.1. Materials. Egg shells were collected from local egg vendors; sucrose (table sugar) was purchased from a local shop, while saw dust was outsourced from a local carpentry establishment. The saw dust was graded using a fine mesh, dried, and stored under dry conditions. Methanol (98% analytical grade) and concentrated sulphuric acid (98%) were purchased from the local chemical supplier. Off-shelf cooking sunflower oil was collected from a disposal point of a selected local supermarket in Kampala city.

2.2. Methods

2.2.1. Preparation of Heterogeneous Base Catalyst. The egg shells were washed with warm distilled water to remove dirt, oven-dried at 100°C for 24 hours [7], and thereafter crushed in a motorized blender (Electromix). About 200 g of crushed shells was calcinated in a muffle furnace (Nabertherm model L5/C6) at different temperature ranges 500–1000°C for 4 hours. The calcinated material (char) was left to cool and then stored in a desiccator.

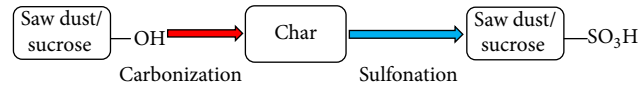

Figure 1: Schematic preparation of saw dust and sucrose acid catalysts. Carbonization process removes volatile compounds like phenols from sawdust producing char; sulfonation adds ($-SO_3H$) group to the char forming carbonized + sulfonated saw dust or sucrose catalyst.

2.2.2. Preparation of Heterogeneous Acid Catalysts. The acid catalysts were prepared from saw dust and sucrose according to Guo et al. [13] with slight modifications. Briefly, the saw dust and sucrose were partially carbonized in a muffle furnace at 400°C under dry nitrogen. The carbonized material (char) was washed with hot distilled water and oven-dried at 105°C for 12 hours.

The resulting material was sulfonated by adding 5 mL of concentrated sulphuric acid (98%) to 5 g of the char and the mixture was placed in an oven at 150°C for 2 hours (Figure 1). The mixture was left to cool and successively washed with hot distilled water until a neutral pH of the wash water was achieved. The material was dried in a hot air oven (Memmert UFE 600) at 105°C for 48 hours, cooled in a desiccator, and stored in dry containers.

2.2.3. FTIR-ATR Spectroscopic Analysis. FTIR spectra of the calcinated egg shells, solid acid catalysts, biodiesel, and regular diesel were obtained in ATR mode with a Perkin Elmer Spectrum Two spectrophotometer equipped with a Universal Attenuated Total Reflectance (UATR) accessory (Version 10.4, USA). The spectrophotometer was run on software NISO2 and different spectra were obtained in the midinfrared region.

For liquid samples, 0.1 mL of sample was spread evenly on the diamond crystal of the ATR to obtain the spectra. Each spectrum was a result of four scans done at a resolution of 4 cm^{-1} over a wavenumber ranging from 4000 to 450 cm^{-1}. For solids, the sample was ground to fine powder using a mortar and pestle and then about 0.01 g of the sample was spread on the diamond ATR crystal. One spectrum was recorded per sample using air as a reference. The diamond crystal was cleaned using a tissue soaked in pure distilled water, between successive sample runs.

2.2.4. Transesterification and Esterification of Sunflower Oil. Transesterification was done according to Dehkhoda and Ellis [12] with slight modifications, using egg shells calcinated at different temperatures. Briefly, 5% (w/w) of the calcinated shell was mixed with 28 mL of methanol and heated to 40°C. The mixture was added to 88 g (100 mL) of oil and heated to 60°C with constant stirring for 120 minutes. The reaction was stopped, residual catalyst sieved off, glycerol decanted off, and biodiesel was washed with hot deionized distilled water.

Esterification was conducted using 1% (w/w) solid acid catalyst, which was mixed with 28 mL of methanol at room temperature, and added to the warm oil (50°C) and gently stirred for 180 minutes. The biodiesel yield was determined from the following equations:

$$\text{Transesterification yield (\%)} = \left(\frac{\text{Weight of refined methyl esters}}{\text{weight of used oil}}\right) \times 100,$$

$$\text{Esterification yield (\%)} = \left(\frac{\text{Initial FFA content} - \text{final FFA content}}{\text{Initial FFA content}}\right) \times 100, \quad (1)$$

where FFA is free fatty acids.

3. Results and Discussion

3.1. Effect of Calcination Temperature on Egg Shells. The FTIR spectra for the eggshells before and after calcinations at 500, 600, 700, 800, 900, and 1000°C are shown in Figure 2. Raw eggshells showed medium bands at 1396 cm^{-1}, 872 cm^{-1}, and 711 cm^{-1} associated with vibrations of carbonate (CO_3^{2-}) groups [11]. The band at 1396 cm^{-1} represented the asymmetric C–O stretch, 872 cm^{-1} represented the out-of-plane bend, and 711 cm^{-1} represented the in-plane bend.

Calcination of egg shells at 500°C eliminated organic matter like protein strands and produced sharp bands at 1402 cm^{-1}, 891 cm^{-1}, and 712 cm^{-1} attributed to calcium carbonate [14]. The intensity of the sharp peaks reduced as calcination temperature increased from 500 to 700°C, possibly signifying the gradual thermal decomposition of carbonate molecules and subsequent emergence of calcium oxide and calcium hydroxide [11].

At temperatures higher than 700°C, there was significant reduction in the carbonate bands, which corresponded to increased rate of decomposition of carbonates [15]. The presence of diminished carbonate bands in egg shells calcinated at 800 and 900°C showed that the transformation into calcium oxide (CaO) was incomplete due to insufficient calcination temperature and time [11].

Conversely, a strong and wide peak corresponding to Ca–O bonds appears in the 500 cm^{-1} region for egg shells calcinated above 700°C (Figure 2(b)). At 1000°C, all the carbonate bands were eliminated due to complete desorption of carbon dioxide from the eggshells, thus producing more basic sites (CaO) that are essential for transesterification to occur [14, 16, 17].

3.2. Effect of Carbonization and Sulphonation on Sucrose. FTIR spectral wave numbers of sucrose (Table 1) reveal variations in the physical structure following carbonization and sulphonation treatments (Figure 3). The spectrum for untreated sucrose (3A) showed three distinct absorption zones at 3500–3000 cm^{-1}, 1500–1280 cm^{-1} and a finger print region 1200–450 cm^{-1}.

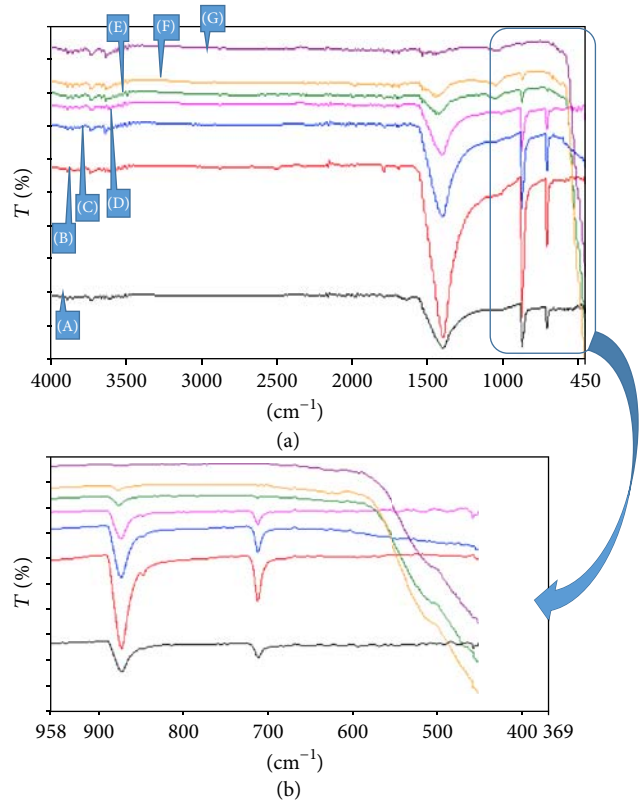

Figure 2: Raw FTIR spectra of eggshells calcinated at different temperatures of 500 (B), 600 (C), 700 (D), 800 (E), 900 (F), and 1000°C (G). Uncalcinated egg shell (A) was used as control. Gradual decomposition of carbonates (a) occurred with increasing calcination temperature, leading to inclinations in spectra of (E), (F), and (G) as seen in (b) due to emergence of calcium oxide bond.

The absorption zone in the 3500–3000 cm^{-1} region corresponded to an O–H vibration and the small peaks next to it represent aliphatic C–H vibrations. The absorption zone in the 1500–1280 cm^{-1} region represented single-bond vibrations of O–C–H and C–C–H, while the intense stretches in the finger print region represent C–O–H and C–O–C vibrations. This spectrum (3A) is similar to that of sucrose reported in previous studies [18, 19].

Subsequent partial carbonization of sucrose (Figure 3(b)) produced a change in spectrum possibly due to loss of bonds in the key regions previously identified in raw sucrose. In particular, reduction in the intensity of the O–H band in the 3500–3000 cm^{-1} region is likely to be a result of the dehydration process leading to loss of O–H bonds due to high carbonization temperature [20]. Carbonization also produced a new peak at 1707 cm^{-1}, corresponding to C=O vibration [21].

The peaks at wave numbers 1590 cm^{-1} and 1420 cm^{-1} most probably correspond to C=C stretches, indicative of aromatic groups. In addition, the C–O stretches and O–H bending vibrations in the 1239–986 cm^{-1} region are significantly diminished probably due to heat. There is broad band also in the 3700–1800 cm^{-1} region that could be a result

Table 1: FTIR spectra represented as wave numbers for untreated sucrose (A), carbonized sucrose (B), and carbonized + sulphonated sucrose (C).

Wave numbers A	Group attributed	Wave numbers B	Group attributed	Wave numbers C	Group attributed
3325	O–H	3333	O–H	2965	C–H
2900	C–H	1707	C=O	1769	C=O
1490	C–C	1590	C=C	1758	C=O
1430	C–O	1420	C=C	1456	C=C
1320	C–O	1239	C–O	1376	O=S
1066	C–OH	986	C–O	1245	$-SO_3H$
1055	C–OH			1057	S=O

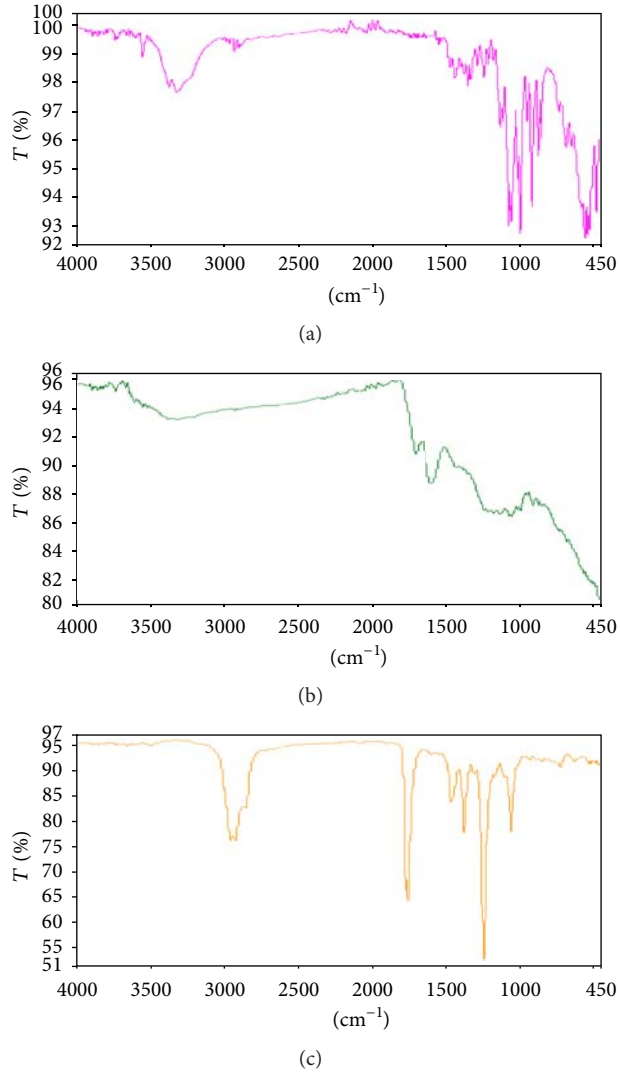

Figure 3: Raw FTIR spectra of sucrose (a), carbonized sucrose (b), and carbonized + sulphonated sucrose (c).

of new hydrogen bonding interactions caused by carbonization, resulting in several oscillation modes in that region [22]. Overall, partial carbonization of sucrose resulted in dehydration and aromatization reactions with subsequent diminution of all major bond peaks previously observed in uncarbonized sucrose [23].

A significant change in the spectrum of carbonized sucrose was observed upon sulphonation with concentrated sulphuric acid (Figure 3(c)). The absence of an O–H peak in the 3000–3500 region indicates total dehydration of the sucrose by the concentrated sulphuric acid [21]. On the other hand, the development of an intense aliphatic peak corresponding to C–H group around the 2900 cm^{-1} wave region was observed.

The vibration of C=O group at wave numbers 1769 and 1758 cm^{-1} intensified possibly due to oxidation and esterification of the abundant O–H groups in sucrose by H_2SO_4. Sharp peaks corresponding to O=S=O group were also observed at 1376 and 1057 cm^{-1}, whereas the intense peak at 1245 cm^{-1} was attributed to the $-SO_3H$ group. The formation of such strong sharp bands indicates that sucrose can easily be carbonized, dehydrated, and sulfonated to facilitate the attachment of catalytic SO_3H acidic groups [24].

3.3. Effect of Carbonization and Sulphonation on Saw Dust. Saw dust on the other hand presented a similar spectrum to that observed in untreated sucrose (Figure 4). There was a broad O–H bond also in untreated saw dust (Figure 4(a)) in the 3000–3500 cm^{-1} region, which could be attributed to cellulose and hemicellulose [25] that are the major carbohydrates in saw dust. A weak C–H vibration was observed at the 2883 cm^{-1} position, confirming the presence of aliphatic groups. Unlike sucrose, a weak C=O peak was observed at the 1727 cm^{-1} region. The region around 1630–1233 cm^{-1} was characterized by weak alkene (C=C), aromatic (C=C), CH_2, and CH groups including phenolic OH groups. The most intense peak at 1032 cm^{-1} could be attributed to C–O vibration. The untreated saw dust spectrum observed here was similar to those seen in previous studies [8, 26].

Carbonization led to the diminution of certain bonds and intensification of others (Figure 4(b)). The most notable was the reduced intensity of the O–H vibration in the 3000–3500 cm^{-1} as well as diminished O–H peak at 1032 cm^{-1}. This reduction in intensity could be attributed to the decomposition of hemicellulose at high carbonization temperatures used in this study. The C=O peaks between 1727 cm^{-1} and

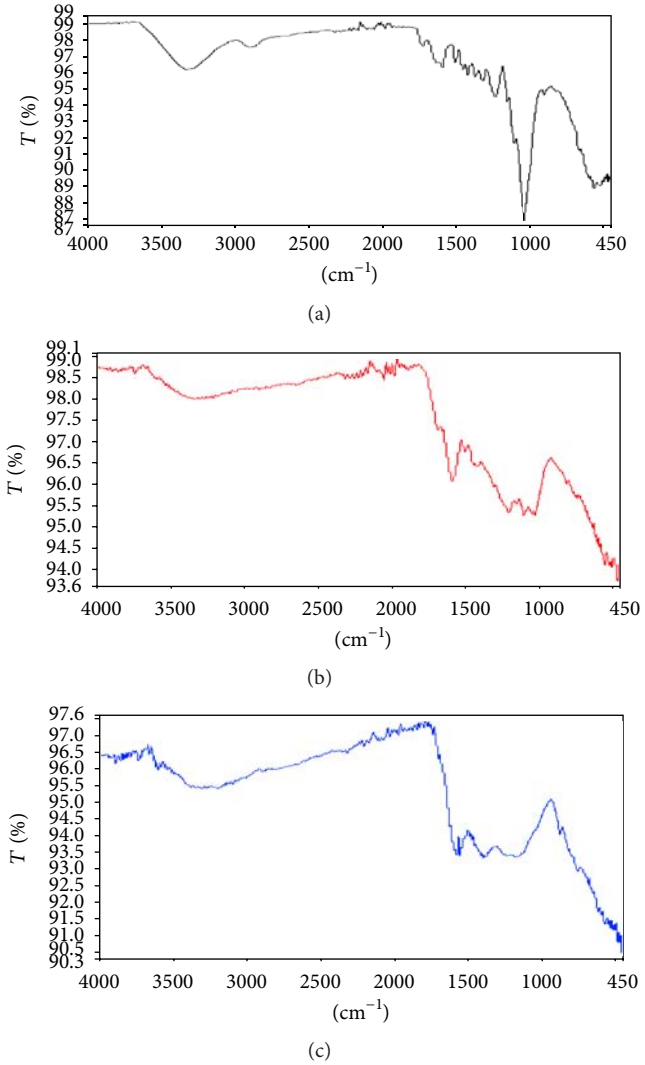

Figure 4: Raw FTIR spectra for dry saw dust (a), carbonized saw dust (b), and carbonized + sulphonated sawdust (c).

1590 cm^{-1} were intensified, indicating increased aromatization due to carbonization [27]. As observed in carbonized sucrose (Figure 2(b)), a broad band in the 3700–1800 cm^{-1} region of carbonized saw dust is likely a result of new hydrogen bonding interactions [22].

Sulphonation of the biochar did not produce significant spectral changes as expected (Figure 4(c)), and, therefore, the spectrum of sulphonated char was similar to that of carbonized saw dust, with minor differences in the 1570–1000 cm^{-1} region. Other than the newly emerged weak band at 1555 cm^{-1}, no bands could be attributed directly to acidic groups as in the case of sucrose spectrum. Other bonds identified in the spectra of raw sawdust, carbonized sawdust, and carbonized sulphonated saw dust are presented in Table 2.

3.4. Transesterification and Esterification of Expired Sunflower Cooking Oil. Single-step transesterification using eggshell

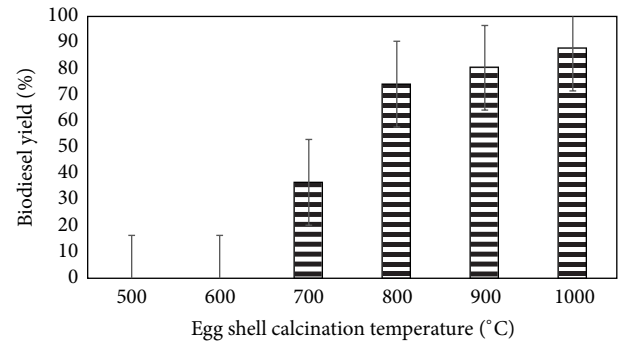

Figure 5: Single-step transesterification of sunflower oil using egg shells calcinated at different temperatures. Experimental conditions: temperature 60°C, methanol/oil ratio 6 : 1, catalyst load 5% (wt/wt), and time 120 minutes.

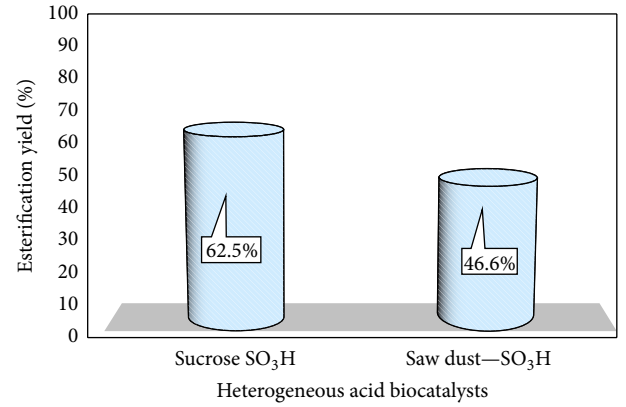

Figure 6: Esterification using heterogeneous acid biocatalysts. Experiment conditions: methanol/oil ratio 6 : 1, temperature 70°C, time 180 minutes, and catalyst load 1% (wt/wt).

calcinated at 1000°C produced the highest yield of biodiesel (87.8%). The lowest biodiesel yield (36.6%) is attained with eggshell calcinated at 700°C (Figure 5). This confirms that calcination temperature of shells has an effect on the final yield of biodiesel attained [28]. The low yield of biodiesel attained with catalyst generated at 700°C is possibly a result of incomplete conversion of $CaCO_3$ to CaO [16, 17], as evidenced by the FTIR spectra (Figure 2).

On the other hand, sulphonated sucrose produced significantly ($p = 0.05$) higher esterification yield (62.5%) than sulphonated saw dust (46.7%) under similar reaction conditions (Figure 6). The high catalytic activity of sulfonated sucrose is likely a result of efficient sulfonation, which could have resulted in a catalyst with higher acid density than that of sulfonated sawdust, which showed no clear evidence of sulfonation (Figures 3(c) and 4(c)). A similar study found that sulphonated sucrose had a higher acid density than all other similarly treated carbons such as starch and lignin [13]. The low activity of saw dust catalyst could be due to incomplete carbonization of lignin in sawdust, leaving excess oxygen in the material which limits the number of $–SO_3H$ groups that could attach onto the carbonized char [13].

Table 2: Wave numbers of FTIR spectra and associated bonds for untreated saw dust (A), carbonized saw dust (B), and carbonized + sulphonated saw dust (C).

Wave number A	Group attributed	Wave number B	Group attributed	Wave number C	Group attributed
3338	O–H	3366	O–H	1555	C=C
2883	C–H	1594	C=C	1397	S=O
1727	C=O	1208	C–O	1155	$S–O^-$
1596	C=C	1106	C–O		
1233	C=C	1028	C–O		
1032	C–O				
559	C–C				

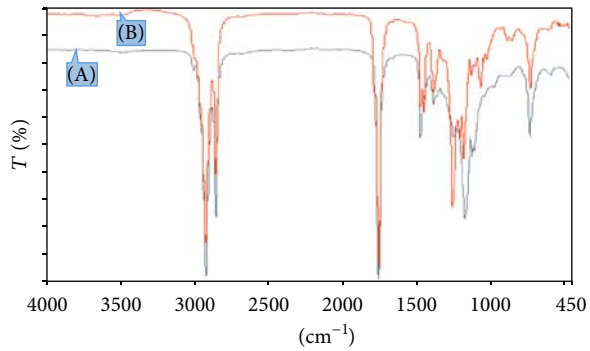

Figure 7: Raw FTIR spectra for expired sunflower oil (A) and biodiesel (B).

4. Characterization of Biodiesel and Regular Diesel Using FTIR-ATR Spectroscopy

FTIR spectra of biodiesel and expired sunflower cooking oil are presented in Figure 7 and the various absorption peaks of biodiesel are presented in Table 3. There were no significant peaks in the regions 1700–2800 cm^{-1} and 3000–4000 cm^{-1} for both expired sunflower cooking oil and biodiesel spectra [29], but both showed strong peaks between 2800 and 3000 cm^{-1} corresponding to C–H vibrations. Major differences between the two spectra lie in the 1500–500 cm^{-1} and are mainly exhibited by esters (biodiesel), as a result of C–O vibrations. The main characteristic peak for biodiesel occurs at 1245 cm^{-1} (C–O) and corresponds to the proportion of fatty acid methyl esters [30]. Other peaks diagnostic for biodiesel were identified at positions 1742 cm^{-1} (C=O) and 1057 cm^{-1} (C–O) similar to those identified in other studies [5, 31].

The spectrum for regular diesel showed some similarities to that of biodiesel, particularly in the 3000–2700 cm^{-1} region (Figure 8). There was also a mild C=O vibration detected in the 1750–1780 cm^{-1} region, unlike the sharp vibration for biodiesel around a similar position as well as a C–O ester diagnostic bond at 1246 cm^{-1}. In contrast, other studies showed no peak in the 1750–1780 cm^{-1} region for diesel [5, 32]. Other peaks for regular diesel are presented in Table 4.

Table 3: Wave numbers responsible for different peaks of biodiesel (BD).

Wave number of BD (cm^{-1})	Group attributed	Vibration type	Absorption intensity
2923	C–H	Stretch	Strong
2880	C–H	Stretch	Strong
2853	C–H	Stretch	Strong
1742	C=O	Stretch	Very strong
1463	$–CH_2$	In-plane bend	Medium
1435	$–CH_3$	Asymmetric bend	Medium
1371	$O–CH_2$	Bend	Medium
1245	$O–CH_3$	Stretch	Strong
1184	C–C	Bend	Weak
1169	C–C	Bend	Strong
1057	C–O	Bend	Medium
722	C–H	Bend	Medium

5. Conclusion

This study established that FTIR-ATR spectroscopy is a quick analytical technique that can be used to confirm the presence of key functional groups on heterogeneous biocatalysts, thus helping to predict activity of catalysts. The FTIR spectra of calcinated egg shells showed gradual decomposition of calcium carbonate with subsequent emergence of calcium oxide as temperature increased. Single-step transesterification of the expired sunflower oil showed that CaO generated from egg shell at 1000°C produced the highest biodiesel yield (87.8%). The spectra for carbonized sulphonated sucrose confirmed the presence of sulphonate ($–SO_3H$) groups, which make the biochar catalytically active, as confirmed by the high esterification yield of 62.5%. Conversely, the sulphonated sawdust showed no clear evidence of the presence of acidic ($–SO_3H$) groups, thus explaining the low esterification conversion achieved with this catalyst. The infrared spectra for biodiesel and regular diesel further help confirm that FTIR-ATR spectroscopy can be rapidly used for final product verification as compared to more costly chromatographic techniques such as HPLC and gas chromatography.

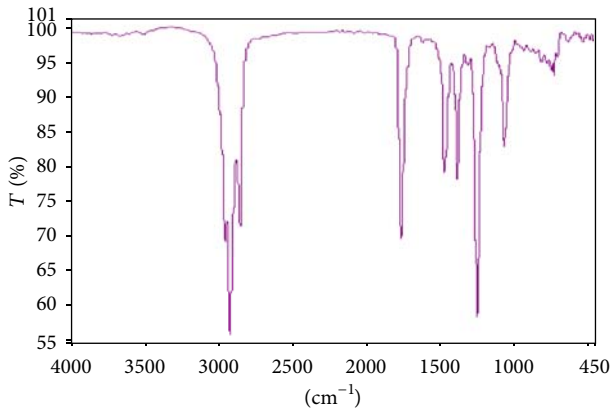

Figure 8: Raw FTIR spectrum of regular diesel.

Table 4: FTIR wave numbers for different peaks of regular diesel.

Wave number diesel (cm^{-1})	Group attributed	Vibration type	Absorption intensity
2954	C–H	Stretch	Strong
2922	C–H	Stretch	Strong
2853	C–H	Stretch	Medium
1770	C=O	Stretch	Medium
1758	C=O	Stretch	Strong
1456	C=C	Stretch	Medium
1376	C=C	Stretch	Medium
1246	C–O	Stretch	Strong
1057	C–O	Stretch	Medium
722	C–H	Out-of-plane bend	Medium

These findings therefore imply that FTIR-ATR spectroscopy may be adopted as an inexpensive alternative for quick analysis of materials and products of chemical reactions.

Conflict of Interests

The authors declare that there is no conflict of interests regarding the publication of this paper.

Acknowledgments

The authors acknowledge financial support from Honorable Justice Simon Byabakama and Mrs Byabakama Dorothy towards this study. This work also received support from the Department of Biochemistry and Sports Science, Makerere University, and the Departments of Chemistry, Microbiology and Biotechnology of Uganda Industrial Research Institute (UIRI), which provided technical as well as infrastructural support to the study.

References

[1] G. E. A. Swann and S. V. Patwardhan, "Application of Fourier Transform Infrared Spectroscopy (FTIR) for assessing biogenic silica sample purity in geochemical analyses and palaeoenvironmental research," *Climate of the Past*, vol. 7, no. 1, pp. 65–74, 2011.

[2] T. Springfield, *Application of FTIR for Quantification of Alkali in Cement*, University of North Texas, Denton, Tex, USA, 2011.

[3] V. A. E. Barrios, J. R. R. Méndez, N. V. P. Aguilar, G. A. Espinosa, and J. L. Dávila, "FTIR—an essential characterization technique for polymeric," in *Infrared Spectroscopy—Materials Science, Engineering and Technology*, T. Theophanides, Ed., chapter 9, InTech, Rijeka, Croatia, 2012.

[4] M. P. Tucker, Q. A. Nguyen, F. P. Eddy, K. L. Kadam, L. M. Gedvilas, and J. D. Webb, "Fourier transform infrared quantitative analysis of sugars and lignin in pretreated softwood solid residues," *Applied Biochemistry and Biotechnology—Part A: Enzyme Engineering and Biotechnology*, vol. 91, no. 1, pp. 51–61, 2001.

[5] M. Bradley, *Biodiesel (FAME) Analysis by FT-IR*, Thermo Scientific, 2007.

[6] B. Stuart, *Infrared Spectroscopy*, Wiley, 2005.

[7] D. J. Holme and H. Peck, *Spectroscopy, Analytical Biochemistry*, Pearson Education, 3rd edition, 1998.

[8] M. Z. Norashikin and M. Z. Ibrahim, "Fabrication and characterization of sawdust composite biodegradable film," *World Academy of Science, Engineering and Technology*, vol. 65, pp. 864–868, 2010.

[9] S. A. Tromp, *ATR-FTIR in catalysis: study of homogeneous, heterogeneous and biocatalysts: TU Delft [Ph.D. thesis]*, Delft University of Technology, Delft, The Netherlands, 2011.

[10] D. Lee, "Preparation of a sulfonated carbonaceous material from lignosulfonate and its usefulness as an esterification catalyst," *Molecules*, vol. 18, no. 7, pp. 8168–8180, 2013.

[11] B. Engin, H. Demirtaş, and M. Eken, "Temperature effects on egg shells investigated by XRD, IR and ESR techniques," *Radiation Physics and Chemistry*, vol. 75, no. 2, pp. 268–277, 2006.

[12] A. M. Dehkhoda and N. Ellis, "Biochar-based catalyst for simultaneous reactions of esterification and transesterification," *Catalysis Today*, vol. 207, pp. 86–92, 2013.

[13] F. Guo, Z.-L. Xiu, and Z.-X. Liang, "Synthesis of biodiesel from acidified soybean soapstock using a lignin-derived carbonaceous catalyst," *Applied Energy*, vol. 98, pp. 47–52, 2012.

[14] N. Tangboriboon, R. Kunanuruksapong, and A. Srivat, "Mesoporosity and phase transformation of bird eggshells via pyrolysis," *Journal of Ceramic Processing Research*, vol. 13, no. 4, pp. 413–419, 2012.

[15] N. Viriya-Empikul, P. Krasae, B. Puttasawat, B. Yoosuk, N. Chollacoop, and K. Faungnawakij, "Waste shells of mollusk and egg as biodiesel production catalysts," *Bioresource Technology*, vol. 101, no. 10, pp. 3765–3767, 2010.

[16] J. Boro, D. Deka, and A. J. Thakur, "A review on solid oxide derived from waste shells as catalyst for biodiesel production," *Renewable and Sustainable Energy Reviews*, vol. 16, no. 1, pp. 904–910, 2012.

[17] A. Jazie, H. Pramanik, A. Sinha, and A. Jazie, "Egg shell as eco-friendly catalyst for transesterification of rapeseed oil: optimization for biodiesel production," *International Journal of Sustainable Development and Green Economics*, vol. 2, no. 1, pp. 27–32, 2013.

[18] L. F. Leopold, N. Leopold, H.-A. Diehl, and C. Socaciu, "Quantification of carbohydrates in fruit juices using FTIR spectroscopy and multivariate analysis," *Spectroscopy*, vol. 26, no. 2, pp. 93–104, 2011.

[19] I. F. Duarte, A. Barros, I. Delgadillo, C. Almeida, and A. M. Gil, "Application of FTIR spectroscopy for the quantification of sugars in mango juice as a function of ripening," *Journal of Agricultural and Food Chemistry*, vol. 50, no. 11, pp. 3104–3111, 2002.

[20] M. Sevilla and A. B. Fuertes, "The production of carbon materials by hydrothermal carbonization of cellulose," *Carbon*, vol. 47, no. 9, pp. 2281–2289, 2009.

[21] M. Liu, S. Jia, Y. Gong, C. Song, and X. Guo, "Effective hydrolysis of cellulose into glucose over sulfonated sugar-derived carbon in an ionic liquid," *Industrial and Engineering Chemistry Research*, vol. 52, no. 24, pp. 8167–8173, 2013.

[22] S. Mopoung, A. Sirikulkajorn, D. Dummun, and P. Luethanom, "Nanocarbonfibril in rice flour charcoal," *International Journal of Physical Sciences*, vol. 7, no. 2, pp. 214–221, 2012.

[23] M. Sevilla and A. B. Fuertes, "Chemical and structural properties of carbonaceous products obtained by hydrothermal carbonization of saccharides," *Chemistry—A European Journal*, vol. 15, no. 16, pp. 4195–4203, 2009.

[24] V. Mirkhani, M. Moghadam, S. Tangestaninejad, I. Mohammadpoor-Baltork, and M. Mahdavi, "Synthesis, characterization and investigation of catalytic activity of a highly sulfonated carbon solid acid in the synthesis of dihydropyrimidinones under solvent-free conditions," *Journal of the Iranian Chemical Society*, vol. 8, no. 3, pp. 608–615, 2011.

[25] R. C. Pettersen, "The chemical composition of wood," in *The Chemistry of Solid Wood*, vol. 207 of *Advances in Chemistry*, pp. 57–126, American Chemical Society, 1984.

[26] G. Müller, C. Schöpper, H. Vos, A. Kharazipour, and A. Polle, "FTIR-ATR spectroscopic analyses of changes in wood properties during particleand fibreboard production of hardand softwood trees," *BioResources*, vol. 4, no. 1, pp. 49–71, 2009.

[27] M. Sevilla, J. A. Maciá-Agulló, and A. B. Fuertes, "Hydrothermal carbonization of biomass as a route for the sequestration of CO_2: chemical and structural properties of the carbonized products," *Biomass and Bioenergy*, vol. 35, no. 7, pp. 3152–3159, 2011.

[28] Z. Wei, C. Xu, and B. Li, "Application of waste eggshell as low-cost solid catalyst for biodiesel production," *Bioresource Technology*, vol. 100, no. 11, pp. 2883–2885, 2009.

[29] S. Choi and Y. Oh, "Evaluation of biodiesel from animal fats by gas chromatography, FTIR spectroscopy and spray behavior," *Advanced Science and Technology Letters*, vol. 58, pp. 133–136, 2014.

[30] N. G. Siatis, A. C. Kimbaris, C. S. Pappas, P. A. Tarantilis, and M. G. Polissiou, "Improvement of biodiesel production based on the application of ultrasound: monitoring of the procedure by FTIR spectroscopy," *Journal of the American Oil Chemists' Society*, vol. 83, no. 1, pp. 53–57, 2006.

[31] T. Yuan, E. Akochi-Koble, D. Pinchuk, and F. R. van de Voort, "FTIR on-line monitoring of biodiesel transesterification," *International Journal of Renewable Energy & Biofuels*, vol. 2014, Article ID 178474, 13 pages, 2014.

[32] A. G. Peña, F. A. Franseschi, M. C. Estrada et al., "Fourier transform infrared-attenuated total reflectance (FTIR-ATR) spectroscopy and chemometric techniques for the determination of adulteration in petrodiesel/biodiesel blends," *Química Nova*, vol. 37, no. 3, pp. 392–397, 2014.